Proceedings of ERAD (2004): 201–205 © Copernicus GmbH 2004

ERAD 2004

Precipitation forecast based on numerical weather prediction models and radar nowcasts

C. Lin, S. Vasić, I. Zawadzki, and B. Turner

Department of Atmospheric and Oceanic Sciences, McGill University, Montréal, Québec, Canada H3A 2K6

Abstract. Radar-based precipitation nowcast methods are robust and have more skill than numerical weather prediction models over time scales of several hours. This is because models do not generally capture the initial precipitation distribution very well. Over longer time scales, the models would perform better than nowcast methods as they resolve dynamically the large scale flow. The eventual goal of this study is to combine precipitation nowcasts with model forecast to yield an optimal forecast. To this end, we first examine the predictability of precipitation based on a model and radar nowcast, using conventional skill scores. We then identify the cross-over point in time where model forecasts start to have more skill than nowcast methods. The final step would consist of a statistical blending of radar nowcasts and model forecasts to produce an optimal forecast.

1 Introduction

For short term prediction of precipitation (0–3 h), nowcast methods based on Lagrangian advection of radar-retrieved precipitation offer the most robust and accurate results at mesoscale resolution, as the initial conditions are known accurately. For longer forecast lead times, numerical weather prediction models may have better predictability, as they resolve the larger scales. This is reflected in the schematic representation shown in Fig. 1, borrowed from Golding (1998), which shows qualitatively the loss of information content in forecasts (i.e. skill) as a function of forecast lead time.

Another issue is that precipitation predictability depends on spatial scale. Germann and Zawadzki (2002) examined the lifetime of precipitation patterns derived from US continental scale radar images from the storm scale to the synoptic scales. They developed a nowcast methodology that combines variational echo-tracking with semi-Lagrangian advection that allows for large scale rotational motion, which is frequently important for the synoptic scales. Skill measures such as the probability of detection (POD), false alarm rate (FAR), critical success index (CSI) and conditional mean absolute error (CMAE) were used to examine four precipitation events. Vasić et al. (2004) compared model and radar-retrieved precipitation using the Canadian and US operational weather prediction models (GEM, ETA) for a 6-day rain event during May 24–30, 2001, which is one of the events studied by Germann and Zawadzki (2002). The radar data are from the US national radar composites. The comparison is done in both physical and spectral space (Fourier and wavelet transform). The agreement between model and radar spectra is satisfactory at the large scales. However, as shown in Fig. 2, models' predicted power spectra decay more rapidly at small scales in comparison with the radar power spectra. In this study, we compare the skill measures of radar nowcasts using the methodology of Germann and Zawadzki (2002) with forecasts from the GEM (Côté et al., 1998) and ETA models. We focus in particular on the cross over point in forecast lead time where the model would perform better than the nowcast, as depicted schematically in Fig. 1.

Correspondence to: C. Lin
(charles.lin@mcgill.ca)

2 Model and radar precipitation

Vasić et al. (2004) examined a 6-day rain event from May 24–30, 2001, comparing the GEM and ETA model 3-hour accumulated precipitation forecasts with radar-retrieved values. Among others, this case is also used in our study. We compare the skill of the radar nowcast (Germann and Zawadzki, 2002) with GEM forecast, over a period of 9 h. Two versions of radar nowcast are considered: a straight unfiltered nowcast (Germann and Zawadzki, 2002) and a nowcast prepared using a "near-optimal forecast filter" (Turner et al., 2004, NOFF). NOFF is designed to optimize forecast correlation and root mean square error statistics through selective filtering of spatial scales based on a wavelet transform. The radar precipitation is taken from US radar composites, a WSI Corporation NOWrad product, with 15 min

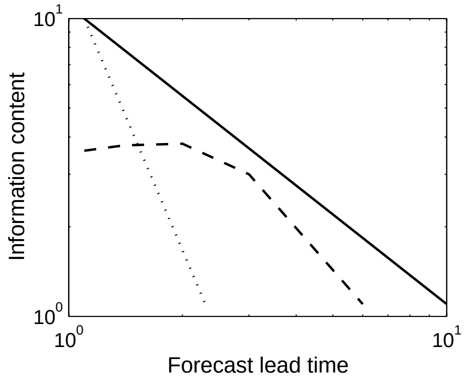

Fig. 1. Schematic representation of the loss of information content in forecasts as a function of lead time. The solid line represents the theoretical limit of predictability. The dashed line represents numerical weather prediction models and the dotted line nowcasting methods. [From Golding (1998)].

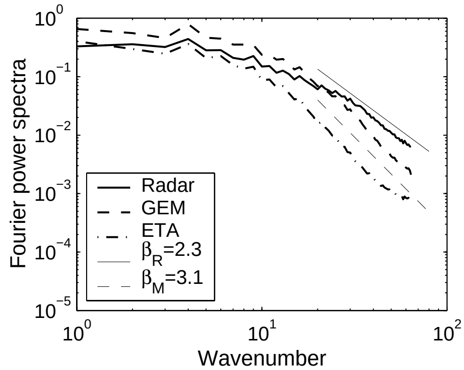

Fig. 2. An averaged Fourier power spectra of the radar observed, and GEM and ETA models' predicted precipitation fields. The estimated spectral slopes β_R and β_M are also shown.

time resolution. The radar data are on a cylindrical equidistant grid with 680×680 points, at the resolution of 4 km. The GEM grid is polar stereographic, with a resolution of 24 km and covering 90×90 points. In some cases we used HIMAP precipitation results, and these results are reported on the resolution of 10 km. The radar data are first projected onto the model grid. Figure 3 shows a typical 3-hour precipitation (mm/3 h) from the radar and radar nowcast (NOWC) on the model grid, the GEM and ETA models' forecasts. The radar-observed precipitation pattern shows significant rotational motion (Germann and Zawadzki, 2002). The GEM and ETA models' precipitation patterns in general resemble the radar-observed pattern, but details are different (Vasic et al., 2004).

3 Precipitation skill measures

We use the skill measures POD, FAR, CSI and CMAE for the evaluation of the model forecast and radar nowcast. The radar precipitation measurements are used for verification. POD, FAR and CSI are categorical measures based on a rain contingency table applied at each analysis grid point over the verification period (Johnson and Olsen, 1998). Z is the number of correct forecasts of rain amount below the threshold, F is the number of false alarms, M is the number of misses, and H is the number of hits or correct rain forecasts. Three thresholds for the precipitation rate for rain cases are used (0.1, 0.5 and 1.0 mm/h). The POD is the number of hits divided by the total number of rain observations, POD=H/(M+H), and gives a simple measure of the fraction of rain events successfully forecast by the model. The false alarm rate is defined as FAR=F/(F+H). It gives a measure of the model's tendency to forecast rain where none was observed. The critical success index (CSI) is the number of hits divided by the total number of hits, misses and false alarms CSI=H/(H+M+F). For the perfect forecast, POD=1, FAR=0 and CSI=1. Following Germann and Zawadzki (2002), we also calculate the conditional mean absolute error (CMAE), which is the domain average absolute error of the forecast at a particular time. For a perfect forecast, CMAE is zero.

4 Comparison of skill scores for model forecast and radar nowcast

We evaluate the POD, FAR, CSI and CMAE for several 9-hour nowcasts, started at 03:00, 06:00, 09:00, 12:00 and 15:00 UTC. In order to have more representative results of the considered precipitation cases, results of these runs are averaged and, in Fig. 4, we refer to the starting time as t=0. Both unfiltered (NOWC) and filtered (NOFF) radar nowcasts, as well as the GEM and ETA model forecasts are performed. The GEM and ETA model forecasts (on the 90×90 grid with 24 km resolution) are verified against radar values projected onto the same grid. As the models' forecasts represent 3-hour accumulations, the skill scores are only available on such temporal resolution. The NOFF and unfiltered nowcast results are very comparable, and we present only the NOWC results. Models' results are given as the dashed lines, and the nowcast results as the solid lines.

In Fig. 4, we present results of the precipitation event of May 25, 2001. First, we focus on the results obtained on the original grid resolution of 24 km which are presented with thinner lines. Both GEM and ETA models perform similarly, and their results are at a fairly steady level over the 9-hour period (dashed lines), according to all four skill scores. The unfiltered 3-hour radar nowcasts start with higher scores (POD above 80%, and FAR near 20%; solid lines) than models, but the skill of the nowcast drops as the forecast lead time increases. At t=7 h, the two POD and CMAE curves cross, indicating the skill of the nowcast has decreased to the same level as the model forecast. However, the skill of the nowcast based on FAR and CSI remains higher compared to the model results throughout the 9 h. The NOFF radar nowcast (not shown) exhibits comparable skill as the unfiltered nowcast for POD, FAR and CSI, but it's CMAE score is better than the unfiltered nowcast. This is expected as NOFF is

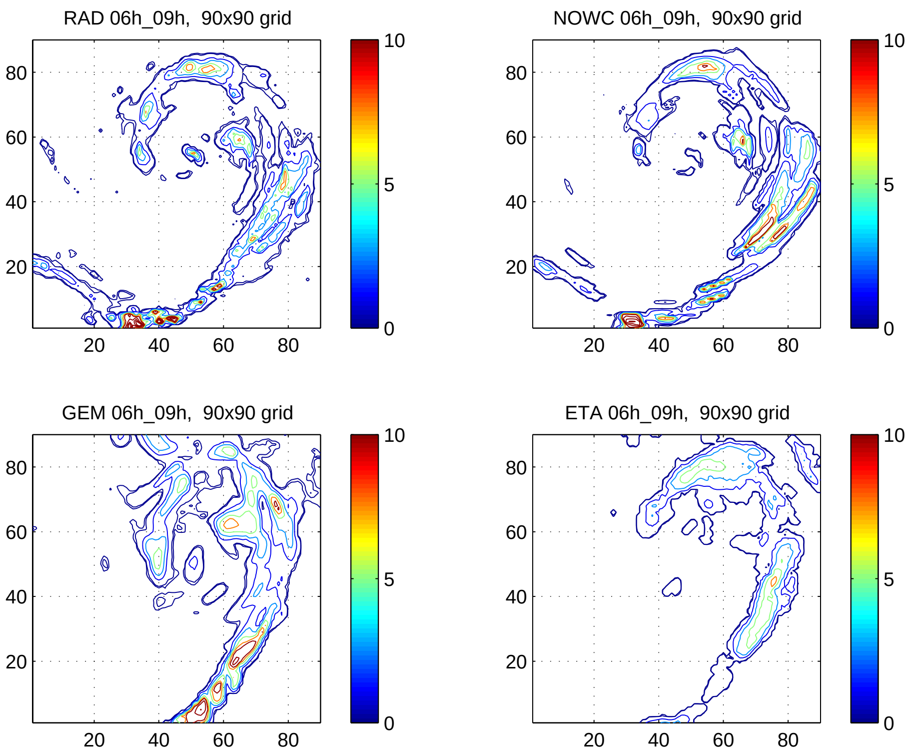

Fig. 3. The accumulated radar (RAD) and radar nowcast (NOWC) precipitation for 06 h–09 h of May 25, 2001 on the model 90×90 grid (top panels), and the GEM and ETA model forecasts (bottom panels). The units are in mm/3h.

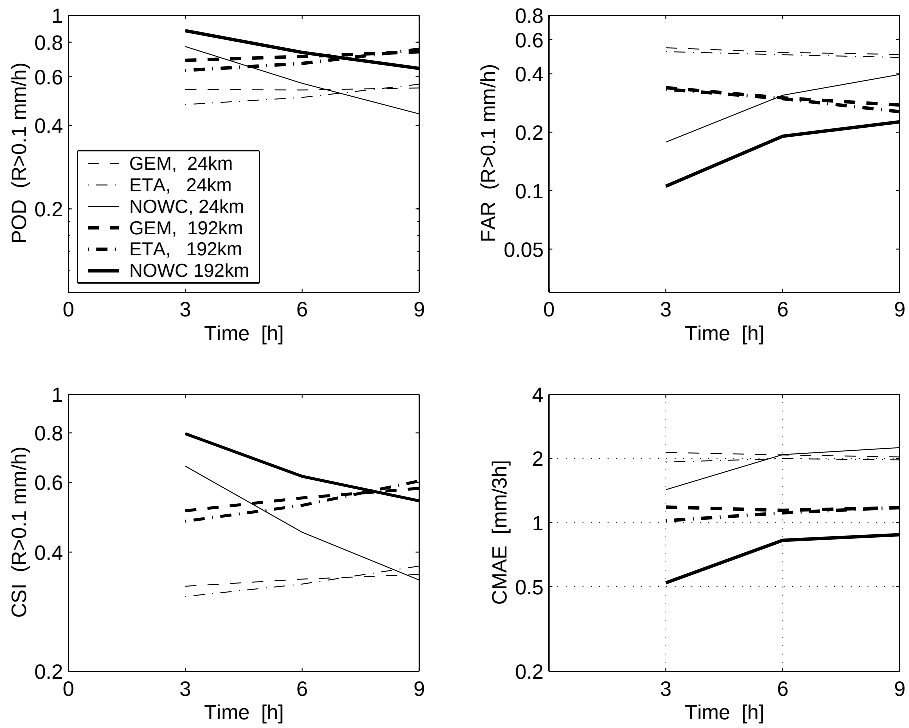

Fig. 4. Average skill scores (POD, FAR, CSI, CMAE) for May 25, 2001 with a threshold of 0.1 mm/h for rainfall rate. Results on the original model resolution of 24 km (thinner lines), and with applied wavelet smoothing function (low-pass filter, with index m=3), representing results on the resolution of 192 km, are shown.

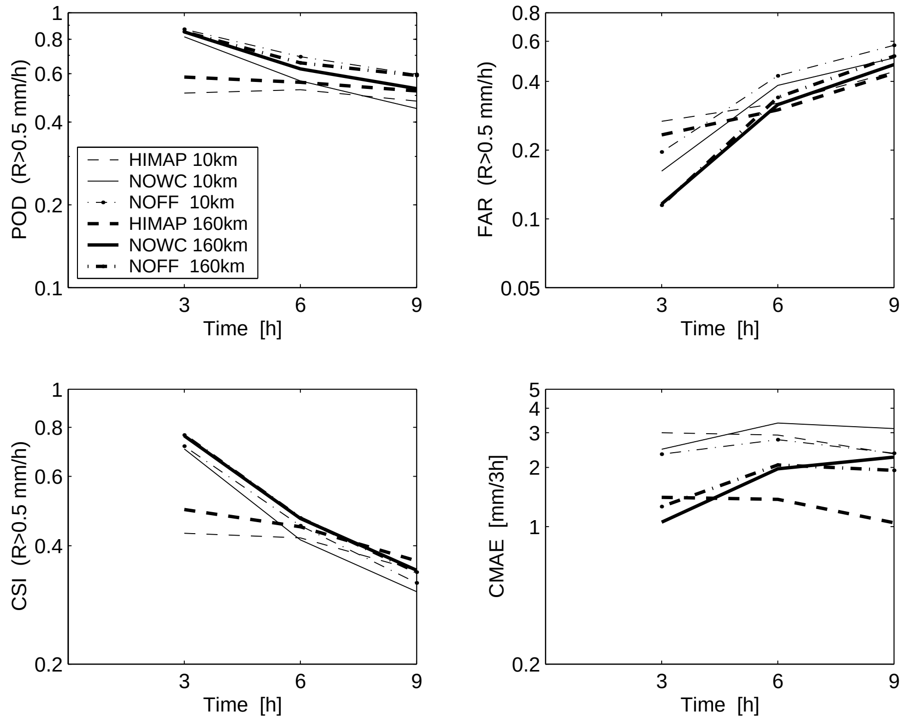

Fig. 5. Average skill scores (POD, FAR, CSI, CMAE) for May 16, 2000 with a threshold of 0.5 mm/h for rainfall rate. Results on the original HIMAP model resolution of 10 km (thinner lines), and with applied wavelet smoothing function (low-pass filter, with index m=4), representing results on the resolution of 160 km, are shown.

designed to minimize root mean square errors. However, as noted by Turner et al. (2004), such filtered nowcasts for long lead times can be visually unsatisfying as the texture of precipitation patterns is lost due to spatial smoothing.

As shown in Fig. 2, models' predicted power spectra decay more rapidly at small scales in comparison with the radar power spectra. Like many other atmospheric fields, precipitation power spectra exhibit the power-law distribution in terms of the associated wavenumbers, $E(k) \sim k^{-\beta}$, (Harris et al., 2001). The higher values of the power-law exponent, β (i.e. the higher spectral slope in the log-log coordinates) are characteristics of a smoother field. In the context of the numerical models, that is attributed to the simplified modelling of the turbulence, and not fully controlled numerical diffusion. Their effect is the largest at smaller scales, and usually present models' results show enhanced falloff of their power spectra on the scales that correspond to ≈5–6 times the horizontal resolution of the computed field. Thus, applying the smoothing function associated with the Haar wavelet transform and Mallat's multiresolution decomposition algorithm (Mallat, 1989), we exhamine skill scores at different scales. The effect of the third low-pass filter (corresponding to scales of 8 times the original grid resolution) is also shown in Fig. 4. Results are presented with thicker lines. Model skill scores are improved. POD and CSI have higher values and FAR and CMAE lower values in comparison with unfiltered values, but the only model cross-over point with the nowcast that is improved is for the CSI skill score.

Results of the second precipitation event of May 16, 2000, are shown in Fig. 5. In this precipitation case, rotational effects are not present and processes are controlled entirely by advection. The medel has better skill score than in the previous case with the rotational effects. Results show that at even higher low-pass filter (with index m=4) than in first case, skill scores are closer to those unfiltered (on the original grid resolution of 10 km). This indirectly implies that the power spectra for this case have less rapid falloff at small scales. Cross-over point in this case occurs somewhat earlier than in the first case.

5 Conclusions

We have shown results of two cases over the continental US where we examine the skill of the Canadian (GEM) and US (ETA) operational forecast models and radar nowcast, over a 9-hour period. The measures used are the POD, FAR, CSI and CMAE. According to all four measures, the radar nowcasts start with high initial skill, but decreases with forecast lead time. The model skill is approximately constant throughout the period. At about 7 h lead time, the radar nowcast has decreased to approximately the same level as the model according to the POD and CMAE scores. We will continue this study with more cases. We will also examine the scale dependence of the predictability using wavelet thresholdings.

Acknowledgements. This work was funded and supported as part of a project of CRTI, an interdepartmental initiative of the Government of Canada.

References

Côté, J., Gravel, S., Méthot, A., Roch, M., and Staniforth, A.: The operational CMC-MRB Global Environmental Multiscale (GEM) model. Part I: Design considerations and formulation, Mon. Wea. Rev., 126, 1373–1395, 1998.

Germann, U. and Zawadzki, I.: Scale dependence of the predictability of precipitation from continental radar images. Part I: Description of the methodology, Mon. Wea. Rev., 130, 2859–2873, 2002.

Golding, B. W.: Nimrod: A system for generating automated very short range forecasts, Meteorol. Appl., 5, 1–16, 1998.

Harris, D., Foufoula-Georgiou, E., Droegemeier, K. K., and Levit, J. J.: Multiscale Statistical Properties of a High-Resolution Precipitation Forecast, J. Hydrometeorology, 2, 406–418, 2001.

Johnson, L. E. and Olsen, B. G.: Assessment of quantitative precipitation forecasts, Wea. Forecasting, 13, 75–83, 1998.

Mallat, S. G.: A theory for multiresolution decomposition, IEEE Trans. on Pattern Analysis and Machine Intelligence, 11, 674–693, 1989.

Turner, B., Zawadzki, I., and Germann, U.: Predictability of precipitation from continental radar images. Part III: Operational nowcasting implementation (MAPLE), J. Applied Meteorology, 43, 231–248, 2004.

Vasić, S., Lin, C. A., Zawadzki, I., Bousquet, O., Chaumont, D., and Vincent, A.: Statistical and scale decomposition analysis of model and radar precipitation, Mon. Wea. Rev., submitted, 2004.